AIAA 2016-3017
Aeroacoustics Conferences
30 May - 1 June, 2016, Lyon, France
22nd AIAA/CEAS Aeroacoustics Conference

Silent Owl Flight: The Effect of the Leading Edge Comb on the Gliding Flight Noise

Thomas F. Geyer*, Vanessa T. Claus†, Ennes Sarradj‡,

Philipp M. Markus§

Brandenburg University of Technology Cottbus - Senftenberg, 03046 Cottbus, Germany

The feathers of owls possess three adaptations that are held responsible for their quiet flight. These are a comb-like structure at the leading edge of the wing, fringes at the trailing edge and a soft and porous upper surface of the wing. To investigate the effect of the first adaptation, the leading edge comb, on the aerodynamic performance and the noise generation during gliding flight, wind tunnel measurements were performed on prepared wings of a Barn owl (*Tyto alba*) with and without the comb. In agreement with existing studies it was found that the leading edge comb causes a small increase in lift. Additionally, at high angles of attack the results from the acoustic measurements indicate that the presence of the comb leads to a reduction in gliding flight noise. Although this reduction is relatively small, it further helps the owl to approach its prey during the final stages of the landing phase.

List of symbols

A_{eff}	[m^2]	effective wing area
ar	[-]	wing aspect ratio
c_l	[m]	averaged chord length
f_c	[Hz]	third octave band center frequency
F_D	[N]	drag force
F_L	[N]	lift force
$h_{s,\text{eff}}$	[m]	effective half span
Ma	[-]	Mach number
L_p	[dB]	sound pressure level
r	[m]	distance
Sr	[-]	Strouhal number based on averaged chord length
U	[m/s]	free stream velocity (flow speed)
x, y, z	[m]	cartesian coordinates
α	[°]	geometric angle of attack

I. Introduction

In 1934, Graham [1] identified three adaptations of the feathers of owls that are held responsible for the quiet flight. These are (1) “a remarkably stiff, comb-like fringe on the front margin of every feather that functions as a leading edge”, (2) a fringe “along the trailing edge of the main wing and of each primary feather” and (3) a fine, short down that covers “certain parts of the upper surface of the feathers”. The existence of these adaptations and their possible effect on the silent flight of the owl has been the subject of several studies in the past. The knowledge regarding the role of the leading edge comb for the noise generation

*Research Associate, Chair of Technical Acoustics, Brandenburg University of Technology Cottbus - Senftenberg.
†Chair of Technical Acoustics, Brandenburg University of Technology Cottbus - Senftenberg.
‡Professor, Chair of Technical Acoustics, Brandenburg University of Technology Cottbus - Senftenberg.
§Master Student, Chair of Technical Acoustics, Brandenburg University of Technology Cottbus - Senftenberg.

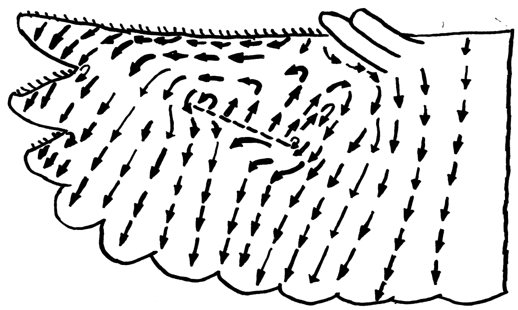

Figure 1. Streamline pattern over the suction side of an owl wing as provided by Kroeger et al. (redrawn from [4])

and the aerodynamic performance of owls is based on only a few, sometimes quite old publications. In some cases, experimental results show a relatively large variance, making it hard to draw a final conclusion.

Mascha [2] examined feathers of different birds and assumes that the special features he found at the feathers of owls, among them an upward-bending of the outer branches on the feathers building the wing leading edge, are responsible for their silent flight. Graham [1] suspects that the main function of the leading edge comb is to locally reduce the velocity of the incoming flow and, additionally, to deflect the flow in a way that it meets the real leading edge under a smaller angle. Hertel [3] states that the leading edge comb affects the boundary layer in a way that the incoming flow becomes turbulent when it passes the hooks. He further assumes that the comb somehow prevents stall and "other acoustically unfavorable processes".

In the 1970s, a number of experimental investigations were performed on flying owls or prepared wings in order to further explore the role of the leading edge comb. For example, Kroeger at al. [4, 5] performed a detailed experimental study on a Florida barred owl (*Strix varia alleni*), with and without the leading edge comb. The owl flew along a certain path inside a reverberation chamber, where measurements were made using a single condenser microphone. Figure 2(a) gives the resulting sound pressure levels obtained from these measurements. The data show a relatively large variance of the results from the same owl with the leading edge comb intact, thus making it difficult to observe a distinguishable acoustic effect of the comb. To draw conclusions on gliding flight aerodynamics, the length of the flight path and the flight time was measured and a lift-drag-ratio of 2.25 was calculated, thus characterizing the owl as a "low performance flyer". Besides the flyover measurements, flow visualization tests were also performed in a wind tunnel on the "wing from a small owl", which had a span width of 0.457 m and a wing area of 0.0465 m^2. The experiments were done using cigar smoke and a tuft probe. At low angles of attack, no effect of the leading edge comb was found, whereas at high angles the comb "developed a vortex sheet which allowed the flow in the boundary layer to be initiated in the outboard direction". Kroeger et al. provided a sketch of the flow field around the owl wing, which is reproduced in Figure 1. It is important to note that, although the flow field is quite complex and consists of areas of counterrotating flow, the flow remains laminar even at very large angles of attack above 30°. When the comb was removed, the areas of counterrotating flow were "replaced by a single large system with the flow being directed inboard at the leading edge". Additionally, with the comb removed flow separation occurred (the flow reattached near the trailing edge) and "considerable turbulence" was observed.

The data provided by Kroeger et al. was later revisited by Anderson [6], who states that the removal of the leading edge comb in Kroegers experiments failed to show a change in flight performance due to the relatively high glide angle in the experiments. He examined the wings of a Great horned owl (*Bubo virginianus*) and concluded that the lift-drag-ratio is much higher than the value given by Kroeger.

Another investigation of the effect of the leading edge comb was included in the study by Neuhaus et al. [7]. They measured the gliding flight noise of a Tawny owl (*Strix aluco*) with and without the leading edge comb using a single microphone and a signal analyzer. Their results are shown in Figure 2(b). Again, the differences are relatively small, and the authors themselves state that they are below the accuracy of the measurement instrument. Additionally, smoke flow visualization experiments were performed on approximately 10 mm wide strips of prepared wings from a Tawny owl and a mallard (*Anas platyrhynchos*). The tests were conducted in a wind tunnel with a flow speed of 3 m/s and an angle of attack of 6°. It was found that the flow around the owl wing is essentially laminar, while large regions of turbulence developed at the pressure side and suction side of the mallard wing. Additionally, a small zone of turbulent circulation

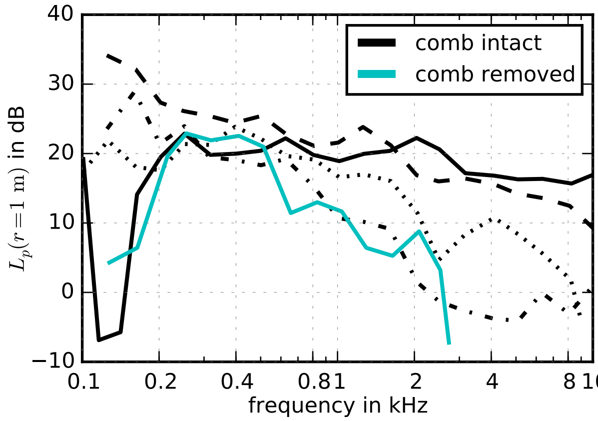

(a) Results from flyover measurements of Kroeger et al. [4] on a Florida barred owl (the data with the leading edge comb intact was derived from four individual measurements of the same bird)

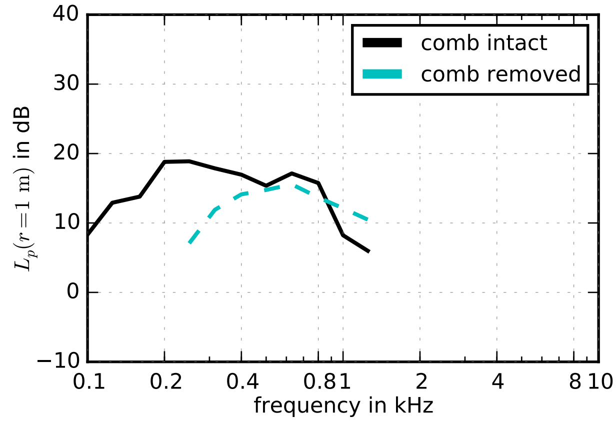

(b) Results from flyover measurements of Neuhaus et al. [7] on a tawny owl

Figure 2. Third octave band sound pressure levels obtained from past flyover measurements of owls with and without the leading edge comb, normalized to a distance of 1 m

was observed near the comb, and it was concluded that it may serve to reattach the flow. When the leading edge comb was removed, the flow around the owl wing was similar to that around the mallard wing, although the regions of turbulence were smaller.

The silent flight of owls was also studied by Lilley in 1998 [8], who revisited the data provided by Kroeger and concludes that the comb stabilizes the flow over the suction side of the wing and prevents laminar separation. Thus, the aerodynamic purpose of the comb is to allow the owl to fly stable at very low speed. Regarding its acoustic effect, Lilley concludes that, by keeping the flow attached, the boundary layer thickness is effectively reduced, leading to a reduced noise generation at the trailing edge.

An extensive work on the special features of the plumage of a Barn owl (*Tyto alba*) was done by Bachmann [9]. This includes three-dimensional scans of the leading edge comb and, as a consequence, a very detailed description of its geometry.

In a recent work by Weger and Wagner [10], the comb-like structures of seven different owl species were examined using a camera, stereo microscopy and a laser-scanning microscope. It was found that comb-like structures of nocturnal owl species featured a larger inclination angle, a larger tip displacement angle and a greater length compared to those of species that are more active during the day. Since nocturnal species are more dependent on their hearing when attempting to capture prey, it was concluded that the serrations have to be involved in reducing flight noise.

Another feature of bird wings that may affect the flight performance and the noise generation, especially in combination with the leading edge comb of the owl, is the so-called alula or bastard wing. It consists of "three or four short feathers that act as a controllable aerodynamic thumb" [6] (see for example Figure 1). In the work of Kroeger et al. [4] this system of feathers, which is located approximately at mid span, is compared to a slat. They state that the combination of the leading edge comb, the alula and the slotted wing tip produces the special vortices that are responsible for the unique flow structures that are developed over the wings of an owl, including the outwards facing flow. Anderson [6] states that during the flight tests conducted by Kroeger et al. the alula was "held slightly open and swept forward". Additionally, he performed flow visualization experiments on airfoil models with and without the presence of a small winglet that acted as an alula. Anderson observed that the winglet delayed stall and developed a vortex field that helped to create the counter-rotating flow pattern described by Kroeger. Bachmann [9] states that the alula is an "anti-stall device" which, when erected, gives the bird additional lift at critical angles of attack, for example during the landing phase of flight.

Concluding this review, it becomes obvious that the available acoustic data either show a relatively large variance or the differences between cases with and without the leading edge comb are simply below the accuracy of the measurement instruments. Hence, a noticeable acoustic effect of the leading edge comb has only been suspected, but is hardly visible in the existing data. Based on the existing literature it seems likely

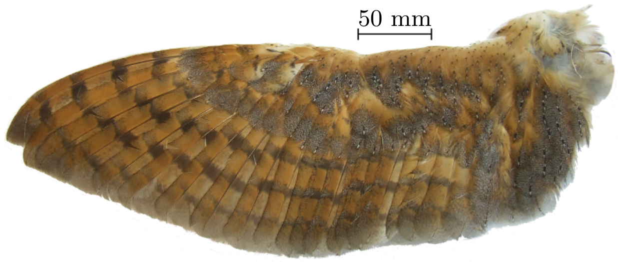

(a) Complete wing

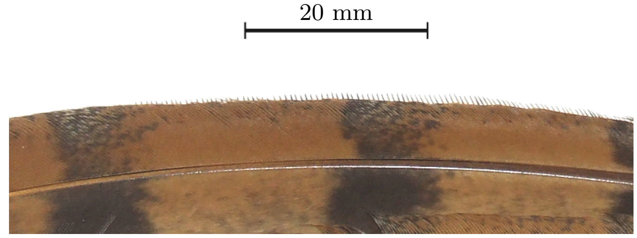

(b) Leading edge hooks

Figure 3. Photograph of a prepared wing used for the experiments (wing 2 from Table 1)

that the comb-like structure at the leading edge of an owl wing, especially in combination with the alula as a vortex generator, merely serves aerodynamic purposes by keeping the flow laminar even at high angles of attack, thus delaying stall.

The present experimental work was motivated by a recent study of the silent owl flight using a set of prepared bird wings [11]. In that work, detailed wind tunnel measurements were performed on wings from two owl species and from three not silently flying bird species. It was shown that the low noise generation of owls is indeed a consequence of their special wing and feather adaptations and not only of their lower speed of flight. However, a question that was not addressed in that investigation was how much each of the single adaptations individually contribute to the silent flight.

Therefore, in the present study the role of the first feather adaptation, the so-called leading edge comb, is investigated by performing wind tunnel measurements on prepared owl wings with and without the comb-like structure. The remainder of this paper is organized as follows: In the following section, the experimental setup is described in detail. This includes microphone array technique, a six-component-force sensor and approaches to investigate the flow field around the owl wing and the deformation of the wing under load. Additionally, preliminary aerodynamic tests using an artificial alula are described. Then, results are presented and discussed. In the last section, the findings of the present study are summarized.

II. Experimental Setup

All measurements took place in the aeroacoustic wind tunnel at the Brandenburg University of Technology Cottbus - Senftenberg using microphone array technique and a six-component force sensor.

II.A. Prepared Wings

In total, measurements were performed on two prepared wings of the Barn owl, which were chosen from a larger set of specimen [11] according to their suitability for the purpose of this study. Figure 3 shows a photograph of one of the wings as well as a detailed photograph of its leading edge comb. The hooks of the comb, which are quite solid barbs with branched tips, were further examined using a Bresser optical microscope with a magnification of 4×, shown in Figure 4.

Both specimens of the present study were left wings, prepared to resemble the wings of an owl in gliding flight with the alula held flush against the wing. As described in [11], the wings are characterized in aerodynamic terms using their effective wing area A_{eff}, their effective half span $h_{s,\text{eff}}$, their averaged chord length c_l and their aspect ratio ar. The effective wing area is the area of that part of the prepared wing that is exposed to the flow, while the effective half span is the spanwise length from the outmost point at the leading edge that is exposed to the flow to the tip of the longest primary feather. The averaged chord length then is determined as the effective wing area divided by the effective half span and the aspect ratio is the ratio of effective half span to averaged chord length. The properties of the wings used for the present study were measured using a Microscribe G2 three-dimensional digitizer and are summarized in Table 1.

In the course of the study, experiments were first conducted using both wings with their leading edge combs intact. The combs were then removed using a scalpel and the experiments were repeated, thus allowing to draw conclusions on the effect of the comb.

Figure 4. Microscope image (magnification 4×) of the hooks from wing 1

Table 1. Properties of the prepared wings used for the present study

Wing	**effective wing area** A_{eff} / $\mathbf{m^2}$	**effective half span** $h_{s,\text{eff}}$ / **m**	**averaged chord length** c_l / **m**	**aspect ratio** ar
1	0.0412	0.31	0.13	2.38
2	0.0391	0.33	0.12	2.79

II.B. Wind Tunnel

The small aeroacoustic wind tunnel at the Brandenburg University of Technology is an open jet wind tunnel [12]. For the experiments on prepared wings, a circular nozzle with an exit diameter of 0.35 m was used. With this nozzle, the maximum flow speed is about 40 m/s, while the turbulence intensity in the core jet (measured at 10 m/s and 15 m/s) remains below 0.2 % [11]. Figure 5(a) shows a photograph of the measurement setup inside the aeroacoustic wind tunnel facility.

For the measurements, the wings were positioned in front of the nozzle (see Figure 5(b)) inside the test section. To this end, they were attached to a three-dimensionally adjustable pan/tilt head, which allows for the adjustment of angle of attack, sweeping angle and flapping angle. As in [11], the geometric angle of attack was measured approximately at the midspan position using an electronic balance held under the wing. The sweeping and flapping angles were kept constant in a way that at zero angle of attack the wing area is approximately level and parallel to the x-y plane (see Figure 5). Surrounding the test section is an anechoic cabin with dimensions of 2.0 m (length) × 1.5 m (height) × 1.55 m (width). It has absorbing side walls, absorbers placed on the floor and a planar microphone array for a ceiling. Thus, the measurement

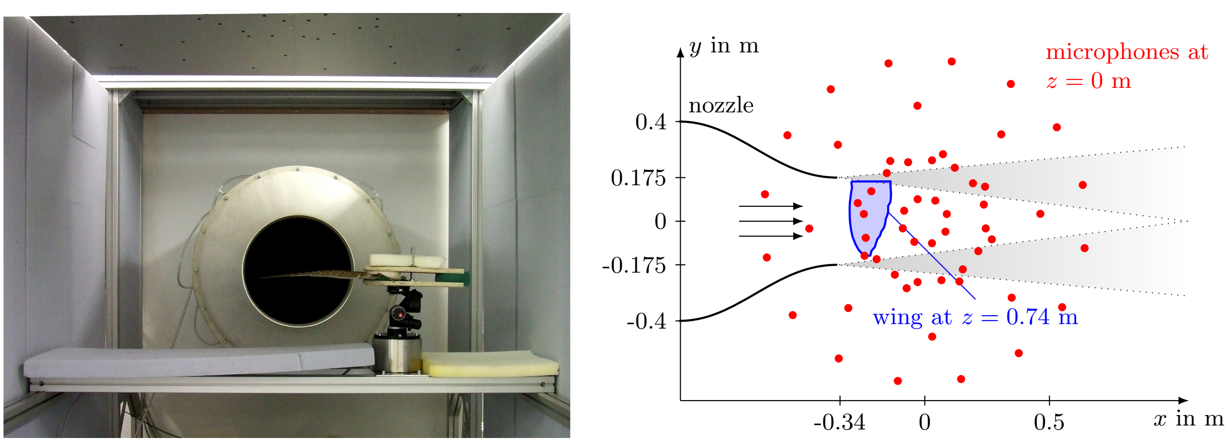

(a) Photograph, taken from downstream

(b) Schematic (top view)

Figure 5. Measurement setup inside the aeroacoustic wind tunnel

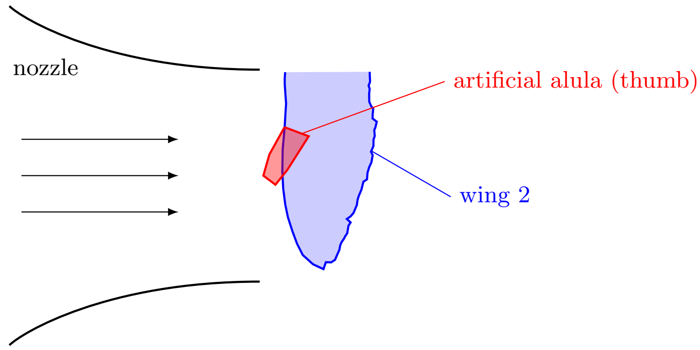

Figure 6. Schematic of measurement setup for tests with artificial alula (thumb wing) attached to wing 2 from Table 1

environment inside the cabin can be described as anechoic for frequencies roughly above 125 Hz.

It is known that owls fly quite slowly, according to [13] their flight speed is only about 2.5 m/s to 7 m/s, while according to [7] it takes values up to 10 m/s. In order to investigate the behavior of the leading edge comb also at higher velocities, flow speeds between approximately 5 m/s and 20 m/s were adjusted in the present measurements.

It is a known effect that the presence of a wing or an airfoil inside an open jet leads to a deflection of the jet and a curvature of the shear layer. As a result, the geometric angle of attack that is adjusted in such a setup is smaller than the so-called effective angle of attack that would be obtained in free flow conditions. Unfortunately, common correction methods like [14] are not practicable for the present case of prepared bird wings, which are highly three-dimensional and cambered. Therefore, the angles of attack of the present study are given to describe different configurations, but they cannot be compared directly to the angle of attack of a freely flying owl.

II.C. Aerodynamic Force Measurements

Aerodynamic measurements were performed on one of the wings using the six-axis sensor *K6D154* made by ME Messsysteme. The sensor measures forces and moments in all three spatial directions. It was positioned inside the test section in a way that the drag force acting on the wing corresponds to the force measured in x-direction, which has a nominal load of 30 N and a measurement uncertainty of ± 0.05 N, while the lift force corresponds to the force measured in z-direction, which has a nominal load of 100 N and a measurement uncertainty of ± 0.15 N. The data were recorded with a sampling frequency of 1 kHz and a measurement duration of 15 s using the amplifier GSV-1A16USB manufactured by the same company. The six-axis sensor provides six voltage signals, which were converted into three forces and three moments by multiplication with the sensor-specific calibration matrix.

When analyzing the aerodynamic data it has to be kept in mind that the angle of attack is adjusted manually by use of an electronic balance which is held under the wing at midspan. Therefore, a certain error of the measured forces due to small deviations of the angle cannot be completely avoided. When adjusted carefully, prior reproducibility measurements showed that the error in lift is below 0.1 N and that in drag below 0.02 N. One exception is the angle of attack of 12°, where at a flow speed around 12 m/s larger deviations in lift of up to 0.2 N occurred. It appears that the wing shape is very sensitive to even slight changes in angle of attack at this point.

In order to obtain at least a basic understanding of the function of the alula, especially in combination with the leading edge comb, a set of preliminary measurements was performed at 20° angle of attack and a constant flow speed of 10 m/s using an artificial alula. This artificial alula was simply cut from cardboard and positioned in the vicinity of the second wing from Table 1. Thereby, the approximate position and dimensions of this device were selected based on photographs of gliding owls and on the available literature [4, 6]. A schematic of the resulting setup is shown in Figure 6. Aerodynamic measurements were then conducted with and without the leading edge comb as well as with and without the artificial alula.

It has to be noted that due to the three-dimensional core jet and the expanding shear layers of the open jet, the aerodynamic forces obtained using the present setup are not directly comparable to values measured in a closed test section.

II.D. Flight Noise Measurements and Data Processing

The noise generated by the prepared wings was measured using a planar 56 channel microphone array, which was positioned outside the flow at a distance of approximately 0.74 m above the wings. In total, 40 s of data were recorded with a sampling frequency of 51.2 kHz. In post-processing the time-data were converted to the frequency domain using a Fast Fourier Transformation (FFT) with a Hanning window on 50 % overlapping blocks of 4,096 samples. The resulting spectra were averaged to yield the final cross-spectral matrix.

As in [11], a CLEAN-SC beamforming algorithm [15] was applied to the measured data, using a steering vector corresponding to Formulation IV in [16]. Thereby, noise sources are assumed to be located within a fully three-dimensional source region. In each spatial direction, the resolution of the focus grid was 0.01 m. The result from this procedure is a three-dimensional mapping of noise sources, a so-called sound map. In order to obtain spectra of the noise generated by the wings, the noise originating from sources located at the wing was integrated. This integration was done using a three-dimensional integration volume that contained only the part of the wing located inside the wind tunnel core jet, but no background noise sources. Finally, the integrated sound pressures were converted to third octave band sound pressure levels.

Due to the fact that the flow speeds are quite low in the present experiments, no correction for the refraction of sound at the shear layer of the open jet was applied.

II.E. Flow Visualization

In order to obtain a qualitative understanding of the flow field around the prepared owl wings, flow visualization experiments were conducted using a tuft probe. It consisted of a thin tuft attached to a holder, which was brought close to the wing surface at different positions on the wing. This provides a very simple method to observe the local direction of the flow, since the tuft will align with the mean flow direction. Additionally, basic conclusions can be drawn on the turbulence of the flow, as the tuft will perform unsteady motions when subject to turbulence and will be immobile when no turbulence is present [17]. The orientation and movement of the tuft was filmed using a handheld camera.

II.F. Estimation of Wing Deformation

Especially at higher flow speeds and angles of attack, the prepared wings will be deformed due to the dynamic pressure of the flow. This deformation has a strong effect on the aerodynamic performance [18]. For example, Kroeger et al. [4] noticed deformations of the wing and found that they are strongly dependent on angle of attack. Significant deformations also occurred in the study by March et al. [19], who measured the lift and drag coefficients of a Great horned owl wing. In order to obtain a rather qualitative measure of the deformation of the prepared wings in the present study, a camera was positioned downstream of wing 1 that captured the wing shape under load. The camera was a CCD monochrome camera that recorded 60 frames per second. Additionally, a common ruler was used to get an estimate of the displacement of the wing tip as a quantitative measure of the wing deformation.

III. Results and Discussion

III.A. Aerodynamic Force Measurements

The resulting lift and drag forces from the aerodynamic measurements are shown in Figure 7(a) and 7(b), respectively. Basically, at each angle of attack the lift force first increases with increasing flow speed up to approximately 12 m/s. With further increasing flow speed, the lift force starts to decrease. This is caused by the deformation of the wing due to the increasing aerodynamic load, effectively leading to a reduction in camber and thus a reduction in lift. The drag force continuously increases with increasing flow speed. Here, the deformation of the wing leads to the fact that, starting at flow speeds above 15 m/s, the drag force reaches the same high values for all angles of attack.

Regarding the effect of the leading edge comb it is visible that without the comb the lift force is lower than with the comb intact. The only exception is at flow speeds below 10 m/s for $\alpha = 20°$ and $\alpha = 24°$. Although the increase in lift due to the existence of the comb is not very large, the effect is significant since it can be observed at nearly all angles and flow speeds. The influence of the comb on the drag force is very small only and more or less within the accuracy of the aerodynamic measurements as described in Section II.C.

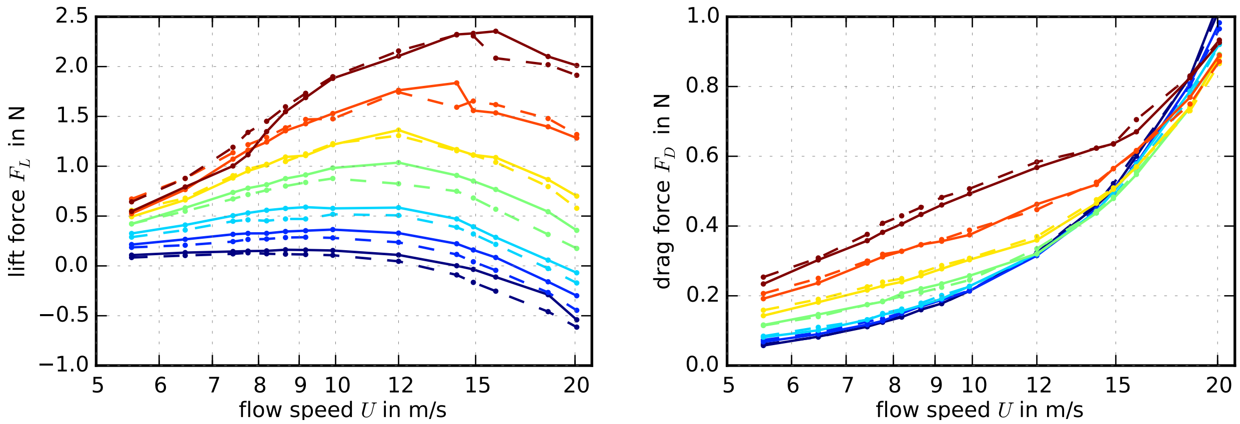

(a) Lift force

(b) Drag force

Figure 7. Lift and drag forces measured for wing 2 from Table 1, solid lines: comb intact, dashed lines: comb removed ($\alpha =$ 0°, 4°, 8°, 12°, 16°, 20°, 24°)

The preliminary tests with the artificial alula (at 20° angle of attack and a flow speed of 10 m/s) revealed that with the leading edge comb intact, the presence of the alula lead to an increase in lift of about 2.4 %, while without the hooks the increase in lift was 1.2 %. These results confirm the assumed role of the alula, although they are more or less only basic estimates, of course. To fully investigate the function of the alula, experiments should be conducted on a larger set of prepared wings with the alula erected and those with the alula held flush against the wing.

III.B. Flight Noise Measurements

Basically, the acoustic data obtained in the present study give evidence that a distinct effect of the leading edge comb can only be found at higher angles of attack. Therefore, results in the present section are only shown for selected angles.

The measured sound pressure levels of the two wings are given in Figures 8(a), 8(c) and 8(e) for angles of attack of 0°, 20° and 24°, respectively. The data are shown as a function of the Strouhal number based on the average chord length c_l of the wings. Following the theoretical scaling of aerodynamic edge noise with the fifth power of the flow speed [20], the sound pressure levels are scaled with Ma^5. At zero angle of attack (Figure 8(a)), no real difference is distinguishable between the cases with leading edge comb and without. At an angle of 20°, small differences are visible, as for example at Strouhal numbers between 5 and 10 the lowest sound pressure levels were clearly measured for the first wing from Table 1 with intact comb. This trend, although not very distinct, continues and becomes more apparent at an angle of attack of 24°.

In order to improve the visibility of the small difference between cases with and without the leading edge comb, the data were filtered using a LOWESS algorithm (*locally weighted scatterplot smoothing*) [21]. The results are shown in Figures 8(b), 8(d) and 8(f), again for angles of attack of 0°, 20° and 24°. It can now be observed that, on average, at zero angle of attack the wings with the comb intact generate the same noise as the wings with the comb removed. At 20° angle of attack, the measured spectra for both wings show a small increase in noise after the comb was removed (although this increase is larger for wing 1). Then, at the highest angle, the results for the first wing show a considerable difference. The sound pressure levels obtained for the wing with the comb intact are in the order of 5 dB below those obtained for the wing with the leading edge comb removed in a large range of chord based Strouhal numbers approximately between 5 and 100. The results for the second wing do not show such differences. If any, the noise generated by the wing without comb is even slightly lower than that generated by the wing with comb at Strouhal numbers from 30 to 80. The reason for these differences between the results for the two wings at this angle are not clear. To fully explore this effect, additional measurements on a larger number of wing specimen would have to be performed.

However, on the whole the sound pressure level spectra shown in Figure 8 indicate that, on average, the leading edge comb does lead to a reduction in gliding flight noise at higher angles of attack, although this has to be described as a rather small scale effect. Nevertheless, it has to be kept in mind that the maximum

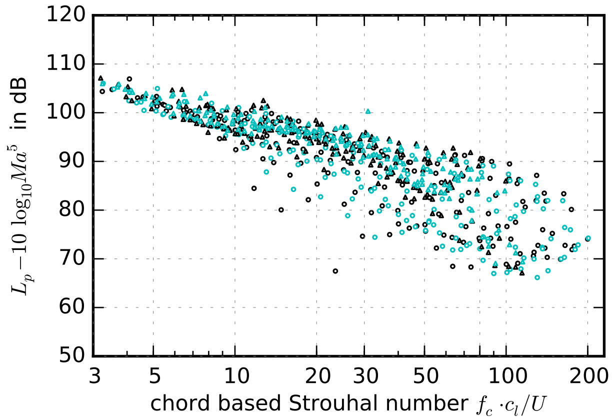

(a) Spectrum at $\alpha = 0°$

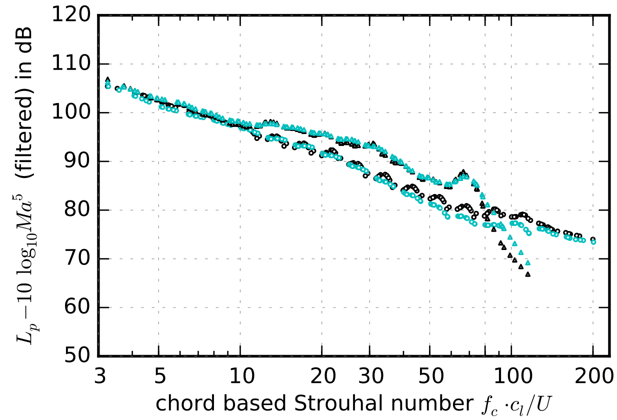

(b) Spectrum at $\alpha = 0°$, LOWESS filtered

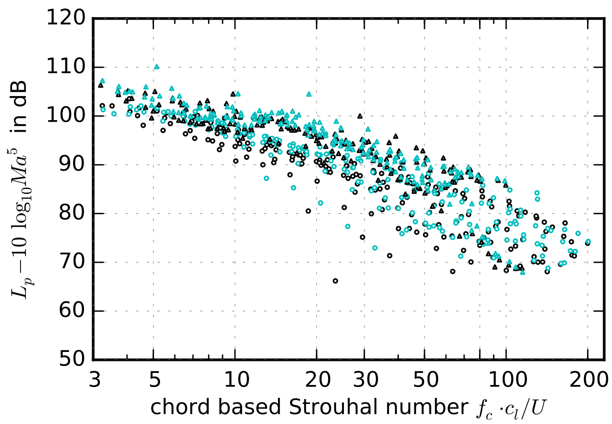

(c) Spectrum at $\alpha = 20°$

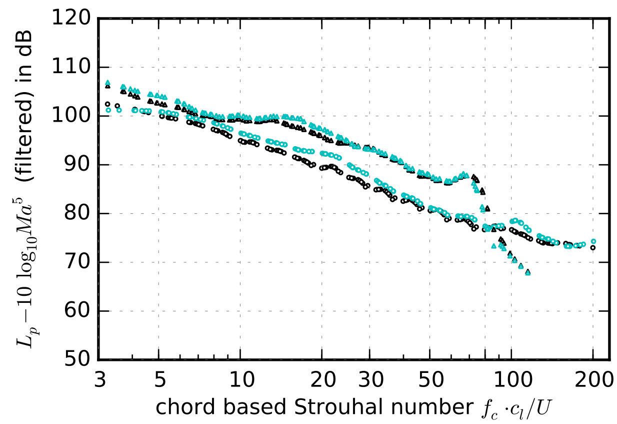

(d) Spectrum at $\alpha = 20°$, LOWESS filtered

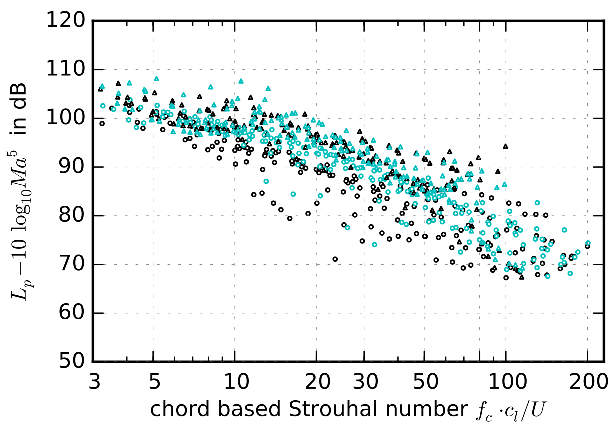

(e) Spectrum at $\alpha = 24°$

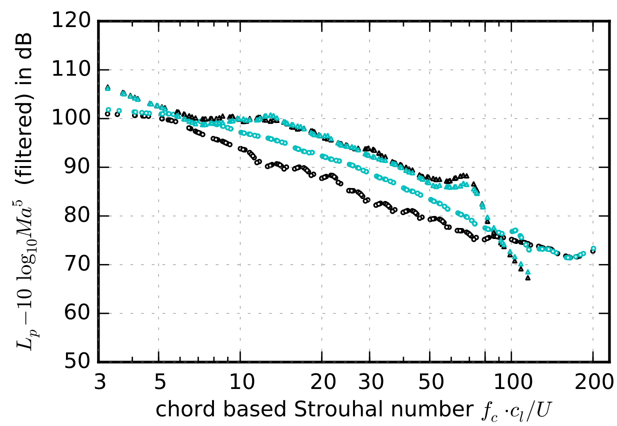

(f) Spectrum at $\alpha = 24°$, LOWESS filtered

Figure 8. Scaled sound pressure levels (black: comb intact, light blue: comb removed) of the two owl wings from Table 1 (circles: wing 1, triangles: wing 2), left column: measured data, right column: data filtered using a LOWESS algorithm [21]

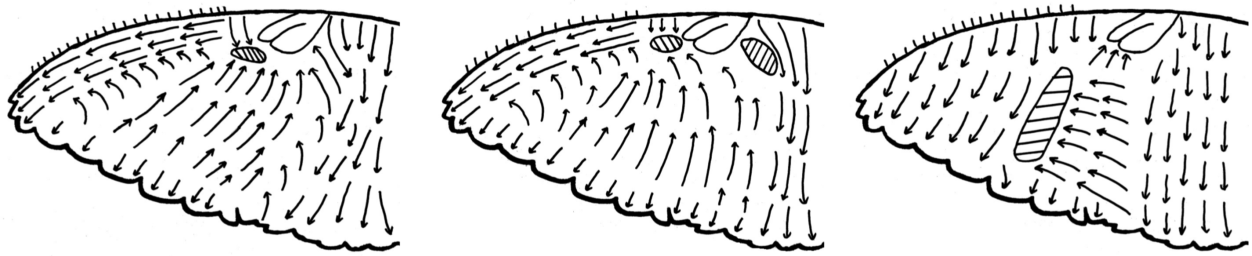

(a) $U = 7$ m/s (b) $U = 10$ m/s (c) $U = 15$ m/s

Figure 9. Results from flow visualization experiments on wing 1 at $\alpha = 24°$ (arrows represent streamlines of the flow over the wing surface, hatched areas represent regions with high turbulence and indistinct flow direction)

geometric angle of attack that can be adjusted with the present experimental setup corresponds to a much lower value under free flight conditions (see Section II.B). Hence, it is possible that the effect shown here continues and even increases at higher angles of attack.

III.C. Flow Visualization

Qualitative results of the flow visualization measurements on the first wing from Table 1 are shown in Figure 9 for three different flow speeds at a geometric angle of attack of 24°. The flow which is directed towards the wing tip was already observed at an angle of 20°, whereas at considerably lower angles this outwards facing flow did not occur. Especially at 7 m/s (Figure 9(a)), the streamline pattern basically resembles the flow field observed by Kroeger et al. [4] as shown in Figure 1. At the highest flow speed of 15 m/s, certain features of the complex flow field, such as the outwards facing flow and parts of the backwards facing flow disappeared and a more regular flow over the wing developed. Somewhat different from the results from Kroeger, however, is the fact that with the comb removed almost the same flow field was observed, only with a much stronger turbulence. This was visible through strong vibrations of the tuft.

III.D. Estimation of Wing Deformation

As a qualitative means to estimate the deformation of the wings due to the dynamic pressure of the flow, Figure 10 shows images recorded with the downstream camera for the first wing from Table 1. For three different angles of attack, the images contain both the wing at zero load (at $U = 0$) as well as under load (at $U = 10$ m/s). A noticeable deformation of the wing is visible, although conclusions regarding a potential effect of the leading edge comb on the deformation are not possible.

Figure 11 then shows the displacement of the wing tip as a function of flow speed. In total, measurements were performed at 7, 10 and 18 m/s. It is visible that at zero angle of attack the wing is bent down towards the pressure side. At positive angles (12° and 24°), the dynamic pressure leads to an upward bending of the wing towards the suction side. Additionally, it was observed that at higher angles of attack the wings were subject to oscillating motions.

Although the accuracy of these measurements is restricted, the results indicate that at higher angles of attack the displacement of the wing tip is slightly higher without the leading edge comb. In combination with the findings from the flow visualization tests, this can be interpreted in a way that the leading edge comb helps to minimize the deformation of the wing and thus to keep the wing shape stable at high angles of attack.

IV. Conclusion

This paper describes a set of experiments that were conducted on two prepared Barn owl wings in order to examine the function of the comb at the leading edge of owl wings. This included acoustic measurements using microphone array technology, measurements of the aerodynamic forces and basic measurements of the wing deformation.

In general, the present investigation yields three main results: Firstly, the comb at the leading edge leads to a small increase in lift, which basically confirms the findings from various studies performed in the

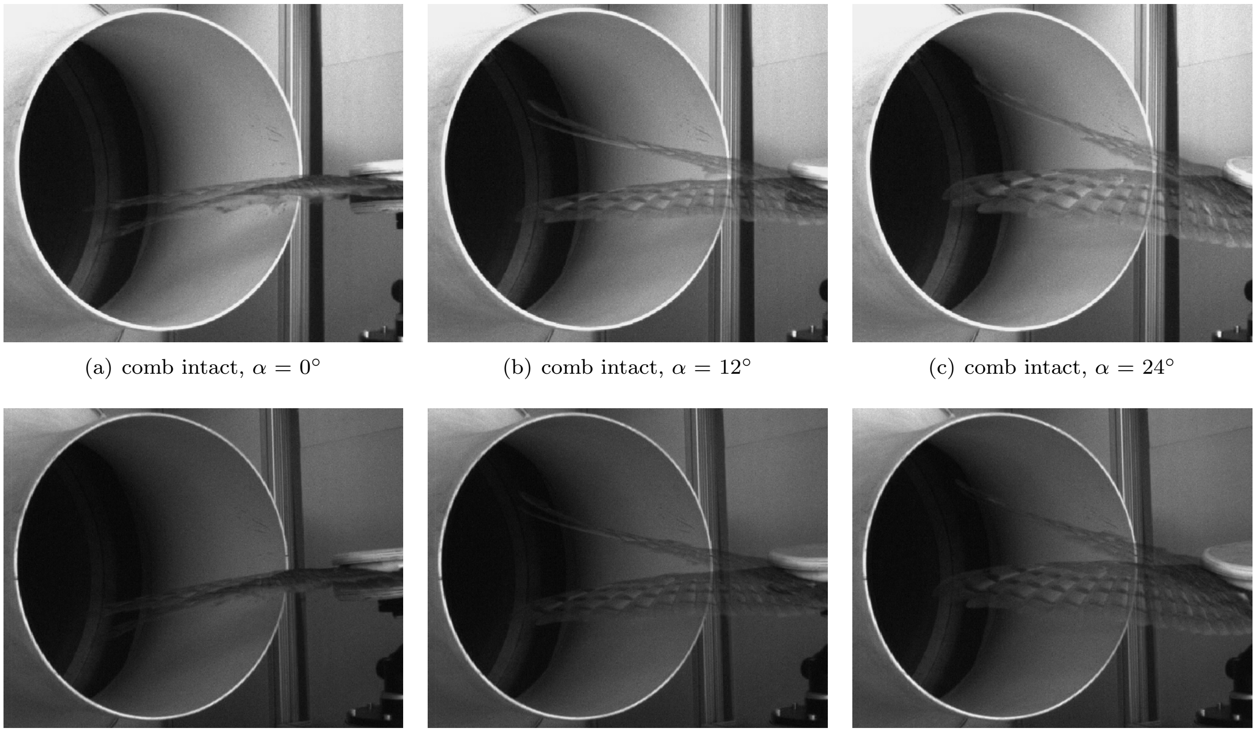

(a) comb intact, $\alpha = 0°$ (b) comb intact, $\alpha = 12°$ (c) comb intact, $\alpha = 24°$

(d) comb removed, $\alpha = 0°$ (e) comb removed, $\alpha = 12°$ (f) comb removed, $\alpha = 24°$

Figure 10. Qualitative results from deformation measurements at wing 1 for different angles of attack, U = 10 m/s, figures are a superposition of photographs with flow (upper wing position) and without flow (lower wing position)

past. Additionally, preliminary measurements using an artificial alula revealed that this device also helps to increase lift, which is again in agreement with past studies. Secondly, the present results suggest that the comb does indeed lead to a small reduction in gliding flight noise at high angles of attack. Usually, the owl increases the angle of attack in such a drastic way only near the end of the gliding flight phase, for example right before attacking its prey. Hence, a noise reduction, although relatively small, at this phase of the gliding flight further enables a nearly silent approach of the owl. Thirdly, the measurements showed that the deformation of the wing is slightly smaller when the leading edge comb is intact. This indicates that the presence of the leading edge comb enables a more steady flight. Since a freely flying owl will have to actively counterbalance strong oscillations and deformations of its wings, this also means that the presence of the comb saves energy.

In addition to the acoustic and aerodynamic measurements, flow visualization experiments were performed using a tuft probe. The resulting sketch of the flow field over the wing at an angle of attack of 24° and a low flow speed (about 7 m/s) resembles the flow field observed in the fundamental study of Kroeger et al. [4].

Acknowledgements

The participation at the 22nd AIAA/CEAS Aeroacoustics Conference 2016 was financially supported by the German Academic Exchange Service *DAAD*, which is gratefully acknowledged. The authors thank Martin Päckert and Jens Ziegler of the *Senckenberg Naturhistorische Sammlungen Dresden* for the preparation of the wings and the helpful discussions.

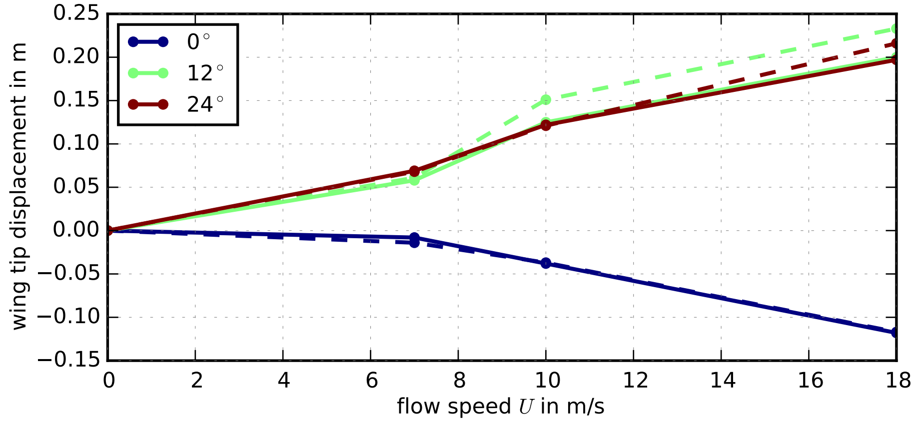

Figure 11. Displacement of the wing tip (solid lines: leading edge comb intact, dashed lines: leading edge comb removed)

References

[1]Graham, R. R., The Silent Flight of Owls. Journal of the Royal Aeronautical Society, 286, 837 - 843 (1934)

[2]Mascha, E., Über die Schwungfedern. Zeitschrift für wissenschaftliche Zoologie, 77, 606 - 651 (1904)

[3]Hertel, H., Struktur, Form, Bewegung. Otto Krauskopf-Verlag Mainz (1963) [translated version: Milton S. Katz (ed.), Structure, Form, Movement. Reinhold, New York (1966)]

[4]Kroeger, R. A., Gruschka, H. D., Helvey, T. C., Low Speed Aerodynamics for Ultra-Quiet Flight. AFFDL TR 971-75 (1971)

[5]Gruschka, H. D., Borchers, I. U., Coble, J. G., Aerodynamic Noise produced by a Gliding Owl. Nature, 233, 409 - 411 (1971)

[6]Anderson, G. W., An Experimental Investigation of a High Lift Device on the Owl Wing. Master's Thesis, Air Force Institute of Technology, Air University, Wright-Patterson AFB, Ohio (1973)

[7]Neuhaus, W., Bretting, H., Schweizer, B., Morphologische und funktionelle Untersuchungen über den 'lautlosen' Flug der Eulen (Strix aluco) im Vergleich zum Flug der Enten (Anas platyrhynchos). Biologisches Zentralblatt, 92, 495 - 512 (1973)

[8]Lilley, G. M., A Study of the Silent Flight of the Owl. 4th AIAA/CEAS Aeroacoustics Conference, Toulouse, France, AIAA paper 1998-2340 (1998)

[9]Bachmann, T., Anatomical, Morphometrical and Biomechanical Studies of Barn Owls' and Pigeons' Wings, PhD-Thesis, RWTH Aachen University (2010)

[10]Weger, M., Wagner, H., Morphological Variations of Leading-Edge Serrations in Owls (Strigiformes). PLOS ONE, 11(3), e0149236 (2016)

[11]Geyer, T. F., Sarradj, E., Fritzsche, C.: Silent Owl Flight: Comparative Acoustic Wind Tunnel Measurements on Prepared Wings. Acta Acustica united with Acustica, Vol. 99, 139 - 153 (2013)

[12]Sarradj, E., Fritzsche, C., Geyer, T. F., Giesler, J., Acoustic and aerodynamic design and characterization of a small-scale aeroacoustic wind tunnel, Appl Acoust, 70, 1073 - 1080 (2009)

[13]Mebs, T., Scherzinger, W., Die Eulen Europas: Biologie, Kennzeichen, Bestände. Kosmos Naturführer (2000)

[14]Brooks, T. F., Marcolini, M. A., Pope, D. S., Airfoil Trailing Edge Flow Measurements and Comparison with Theory incorporating Open Wind Tunnel Corrections. 9th AIAA/NASA Aeroacoustics Conference, AIAA paper 84-2266 (1984)

[15]Sijtsma, P. CLEAN based on spatial source coherence. International Journal of Aeroacoustics, 6(4), 357-374 (2007)

[16]Sarradj, E.,Three-dimensional acoustic source mapping with different beamforming steering vector formulations. Adv Acoust Vib, Vol. 2012 (2012)

[17]Merzkirch, W., Techniques of flow visualization. No. AGARD-AG-302, Advisory Group for Aerospace Research and Development Neuilly sur Seine, France (1987)

[18]Knappe, H., Wagner, S., Die aeroelastische Deformation von Vogelflügeln und ihr Einfluss auf die Profilpolaren. In: Nachtigall, W. (ed.): BIONA-Report 3. Akad. Wiss., Mainz: G. Fischer, Stuttgart, New York, 25 - 44 (1985)

[19]March, A., Bradley, C., Garcia, E., Aerodynamic Properties of Avian Flight as a Function of Wing Shape. ASME International ME Congress and Exposition, Orlando, FL (2005)

[20]Ffowcs Williams, J. E., Hall, L. H., Aerodynamic sound generation by turbulent flow in the vicinity of a scattering half plane, Journal of Fluid Mechanics, 40, 4, 657 - 670 (1970)

[21]Cleveland, W. S., Robust locally weighted regression and smoothing scatterplots. Journal of the American Statistical Association, 74, 829-836 (1979)